Preliminary report on the Lesvos 12 June 2017 M_w=6.3 earthquake

Papadimitriou P., Tselentis G.A., Voulgaris N., Kouskouna V., Lagios E., Kassaras I., Kaviris G., Pavlou K., Sakkas V., Moumoulidou A., Karakonstantis A., Kapetanidis V., Sakkas G., Kazantzidou D., Aspiotis T., Fountoulakis I., Millas C., Spingos I., Lekkas E., Antoniou V., Mavroulis S., Skourtsos E., Andreadakis E.

Faculty of Geology and Geoenvironment, National and Kapodistrian University of Athens

Introduction

The Aegean Region is one of the most active seismically parts of the Alpine-Himalayan Mountain Belt. The Aegean microplate is bounded by the western extension of the North Anatolian Fault to the north and the Hellenic Trench to the south (McKenzie, 1978; Mercier et al., 1989). NE Aegean is a well-known zone of active crustal extension, located south of the right-lateral North Anatolian Fault Zone (NAFZ), and above the Hellenic Trough where the oceanic lithosphere of Tethys is subducted under the Aegean continental one (e.g., Ketin, 1948; McKenzie, 1972, 1978; Dewey and Şengör, 1979; Le Pichon and Angelier, 1979, 1981; Şengör et al., 1985).

GPS measurements and earthquake slip vectors revealed that the relative plate motions along the NAFZ (25 mm/yr W) and across the Hellenic Trench (40–50 mm/yr SW) cause diffuse extensive deformation in the back-arc region (Dewey and Sengör, 1979; Barka and Reilinger, 1997). The anomalously low elevated extension that prevails in the Aegean allows Anatolia to move with increasing velocity to the WSW, leading to the westward opening of Izmir Bay, which is bounded by parallel E-W striking normal faults (Mascle and Martin, 1990).

Several studies carried out by Hecht (1972, 1974a,b), Pe-Piper (1978), Katsikatsos et al. (1982, 1986), and Pe-Piper and Piper (1993) described the geology and provided the geological maps of Lesvos Island (Figure 1). The geology can be summarized as a basement composed of Alpine and pre-Alpine metamorphic rocks which were then covered by post-Alpine formations such as Miocene volcanic rocks and Neogene marine and lacustrine deposits (e.g. Migiros, 1992; Soulakellis et al., 2006). More specifically, Lesvos Island consists of an autochthonous and allochthonous unit as well as post-Alpine formations. The autochthonous unit consists of a series of upper Paleozoic formations over upper Triassic. It also consists of metaclastics, with lenses and interbedding of crystalline limestones and dolomites. The allochthonous units are separated mainly in two tectonic nappes: a) lower Triassic volcano-sedimentary formations and b) lower ophiolithic rocks.

The tectonic evolution of Lesvos Island is affected by the general neotectonic evolution of the Aegean, which started in the Oligocene (15 Myr). Tectonic analysis of faults and microruptures of Lesvos Island (Hecht, 1974; Katsikatsos et al., 1982) revealed three main fault systems with the strike N40°-60°W, N30°-60°E and E-W, respectively. The NE oriented fault system prevails at the NE part of the island, while fault zones of NW and E–W direction are parallel to the orientation of the coast. The respective E-W trending faults appear to be the oldest structures in the area.

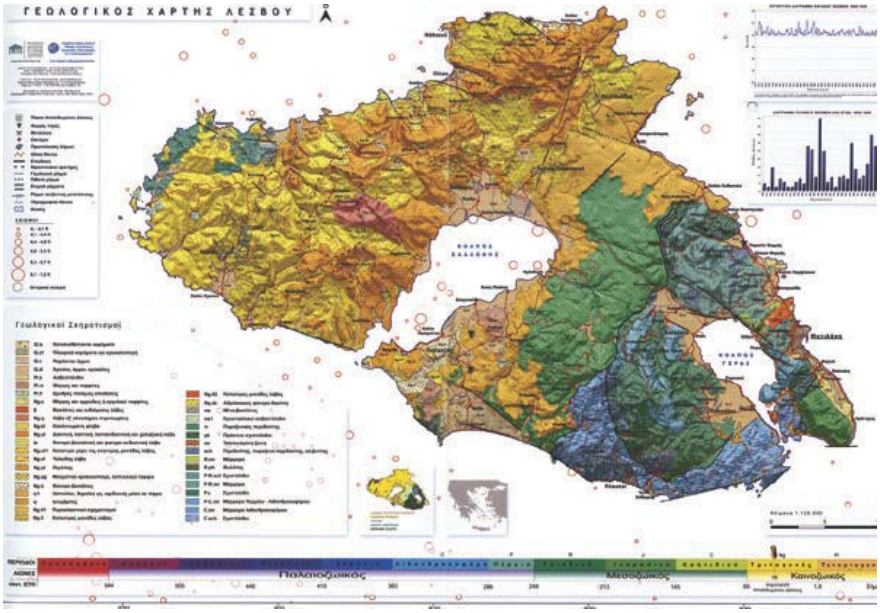

Figure 1: Geologic map (IGME; Hecht, 1974; Katsikatsos et al., 1982; Migiros, 1992; Soulakellis et al., 2006)

The region of Lesvos and Chios Islands, in the NE Aegean, has suffered from several strong and destructive earthquakes since the antiquity, as well as during the 20th century (Papazachos and Papazachou, 2003; Makropoulos et al., 2012; Stucchi et al., 2013). High seismic activity of Lesvos is related to the neo-volcanic rocks. According to Voulgaris et al. (2004), foci of Lesvos Island are shallow ($h \leq 50$ km) and concentrated in three zones. The first seismic zone crosses the north coast of Lesvos (magnitude of 6.0 – 7.0). The second seismic zone crosses the south and southeastern coast of Lesvos Island (magnitude of 5.0 – 6.0). The third seismic zone crosses the SW part of Lesvos with a NW orientation (magnitude ≤ 5.5). This is the most active fault zone on Lesvos Island (Delibasis and Voulgaris, 1989).
According to Papazachos and Papazachou (2003), the first reported historical event in Chios (M=6.2) occurred in 496 B.C., while in Lesvos (M=6.8, I=X) in 231 B.C. (M=6.8, I=X). Following, in 1383 an M=6.8 (I=IX) earthquake took place west of the northern coasts of Lesvos Island, destroying Mytilene and killing 500 people. On 7 March 1867 a destructive earthquake (M=6.8, I=X) occurred in Lesvos island. It destroyed the capital and many houses in the country. It killed 550 people and injured 816. Ground fissures, liquefaction phenomena and landslides were also observed. The 25 October 1889 Lesvos M=6.8 earthquake destroyed the western part of the island, killing 36 people, destroying 1800 houses and causing rockfalls.

The historical event that presents most similarities with the 12 June 2017 (Figure 2) earthquake is the one that occurred on 11 October 1845 (M=6.7, I_{EMS98}=8.5) (Taxeidis, 2003). In Vrissa, 60 houses were destroyed and a woman was killed due to landslides caused by the intense aftershock sequence. In Plomari 8 houses were destroyed, while 40 were damaged. Other areas of the island were heavily damaged, as in Vivari, where many houses and the local church almost collapsed, and in Lisvori, where only 2 out of the 70 or 80 houses did not collapse (Papazachos and Papazachou, 2003). This repeatability of the seismic effects infers local soil conditions that may have triggered local site amplifications of the seismic waves.

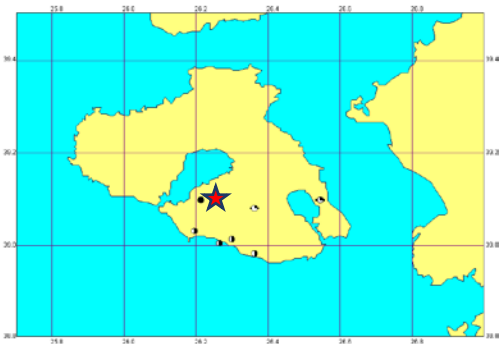

Figure 2: Epicenter and MDP's of the 1845 earthquake (Taxeidis, 2003).

Concerning instrumental seismicity (since 1900) most events are located offshore between Lesvos and Chios Islands and towards the western coast of Turkey. On 18 November 1919, an Ms=7.0 (Makropoulos et al., 2012) occurred close to the western coast of Turkey south of Lesvos, causing severe damage in Mytilene, whereas the Ms=7.0 22 September 1939 event occurred north of Lesvos. On 23 July 1949 an Ms=7.0 offshore event (I=IX) occurred NE of Chios Island (Figure 3). 49 settlements were destroyed in Chios, where 534 houses collapsed, 2526 were seriously damaged and 2985 slightly (Papazachos and Papazachou, 2003). In Kardamyla (N. Chios) only 7% were not destroyed, 3 persons were killed and 50 injured. Fissures in the ground and rockfalls were observed in the north part of Chios. In the capital of Chios 99 houses collapsed, the dock was fissured and in many places the ground suffered landslides.

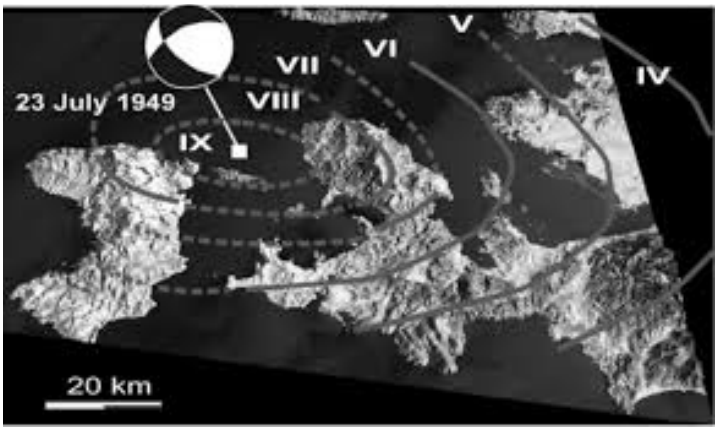

Figure 3: Isoseismal Map of the 23 July 1949 earthquake as modified from Erkman (1949). Focal mechanism solution indicating normal faulting from Eyidogan (1988) (Altinok et al., 2005).

The 12 June 2017 (M_w=6.3) Lesvos earthquake sequence

On 12 June 2017 (12:28 GMT) an offshore destructive earthquake occurred approximately 15 km south of the SE coast of Lesvos Island, NE of Chios. There was one fatality in Vrissa village, caused by building collapse and fifteen people were injured. Landslides and surface ruptures caused temporary blockage of the road connecting Plomari with Melinta, along the southeast coast of Lesvos. The access of the road is denied until the end of the aftershocks activity. Coseismic low tide effects accompanied by high tide ones immediately after the main-shock were documented in the port of Plomari. Damage was widespread throughout the island (damage is reported in at least 12 villages) whereas effects have been also observed at the Turkish coast. During the first round of buildings' formal inspections of 583 buildings, 337 were found unsafe for use. Heaviest damage was reported in the village of Vrissa (Figure 4). About 80% of its buildings, most of them traditional stone masonry residential constructions built by the end of the 19th century were damaged. Several collapsed while many were heavily damaged, reported dangerous and/or unrepairable. Monumental constructions, such as post-Byzantine churches suffered serious static effects. Wall cracks have been also observed at several old buildings in the historical centre of the capital town of Mytilene, located about 35 km NE of the epicenter. Among these are the buildings of the University as well as the historical town hall of the city. Old industrial buildings in several villages up to 35km from the epicenter presented also partial collapse.

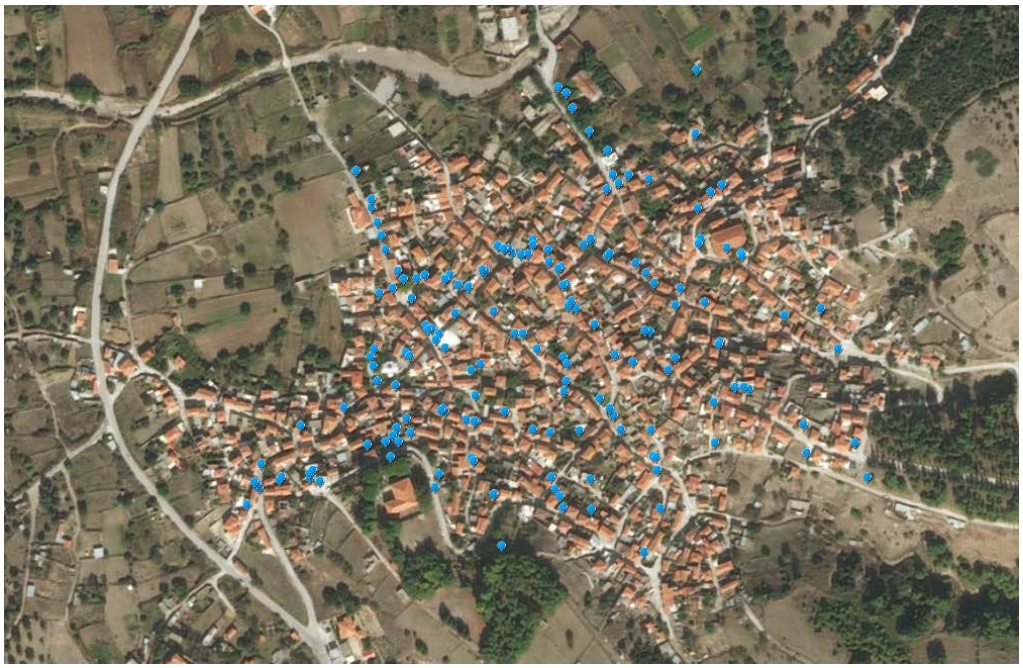

Figure 4: Vrissa Settlement. Blue marks, which indicate damaged buildings, were collected a day after the earthquake (http://arcg.is/2sjqRNv) by a field team of Dynamic, Tectonic, Applied Geology Department of NKUA who moved to the area.

The epicenter of the mainshock was automatically determined by the Seismological Laboratory of the National and Kapodistrian University of Athens (NKUA-SL) and the solution was promptly available online for the public (www.geophysics.geol.uoa.gr/stations/maps/recent.html). Manual analysis was performed for the mainshock and for the aftershocks the aftershocks of the first three days of the rich sequence (Figure 5). The spatial distributions of the aftershock sequence is concentrated offshore south of the SE coasts of Lesvos Island. The epicentres are aligned along an approximate NW-SE direction, covering an area of about 30x10 km^2.

Taking into account the automatically located epicentre of the SL-NKUA, the real time PGA distribution was obtained considering the magnitude, the soil category and the type of the focal mechanism reaching a maximum value of 200 cm/sec^2 in South Lesvos (http://macroseismology.geol.uoa.gr/realtime).

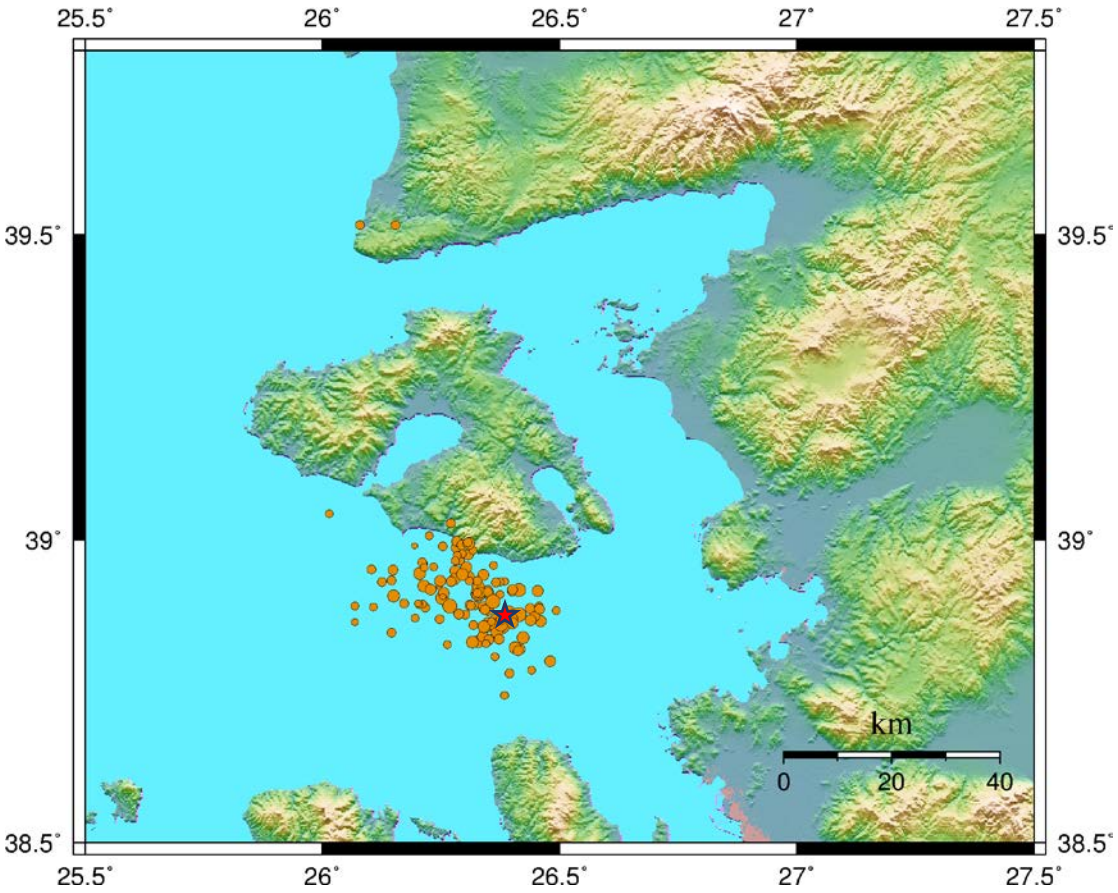

Figure 5: Aftershocks distribution of the largest events.

Regional moment tensor inversion was applied for the focal mechanism determination of the mainshock and the major aftershocks of the sequence. The frequency-wavenumber integration method (Bouchon, 1979, 2003) was used to calculate Green functions. Afterwards, synthetic waveforms are generated and compared with the observed ones for a given velocity structure, as described by Papadimitriou et al.

(2012). The developed methodology was successfully applied (Papadimitriou et al., 2015) in other regions, such as Santorini, during the 2011-2012 seismic crisis (Kaviris et al., 2015).

The seismic moment of the mainshock, located at a depth of 13km, was calculated $M_0=3.5\cdot10^{25}$ dyn·cm and the determined focal mechanism indicates normal type faulting with the fault plane oriented in a NW-SE direction (φ=293º, δ=50º and λ=-96º), (Figure 6). Fault plane solutions of the largest aftershocks (3.9≤Mw≤4.6) have also been determined, indicating a similar type of faulting, and are published in the website of the Seismological Laboratory of the University of Athens (www.geophysics.geol.uoa.gr). The focal mechanism of an aftershock is presented in Figure 7.

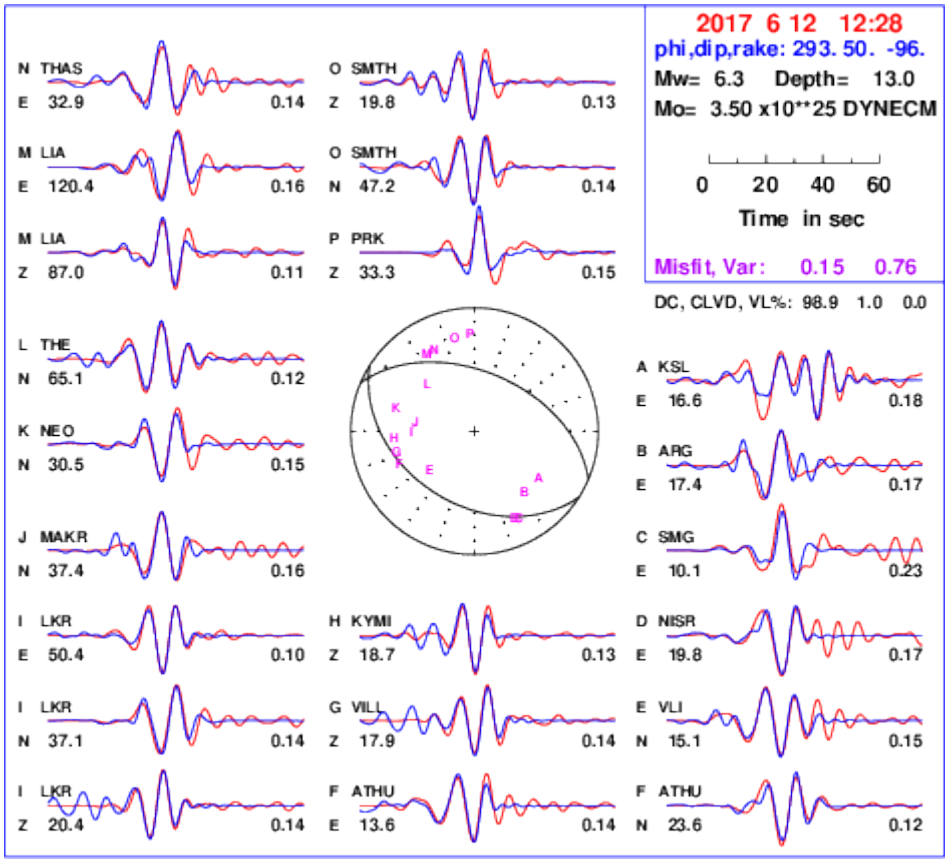

Figure 6: Source parameter determination for the 12 June 2017 Lesvos mainshock, using moment tensor inversion and recordings in local and regional distances. Red and blue colour lines represent the observed and synthetic waveforms, respectively.

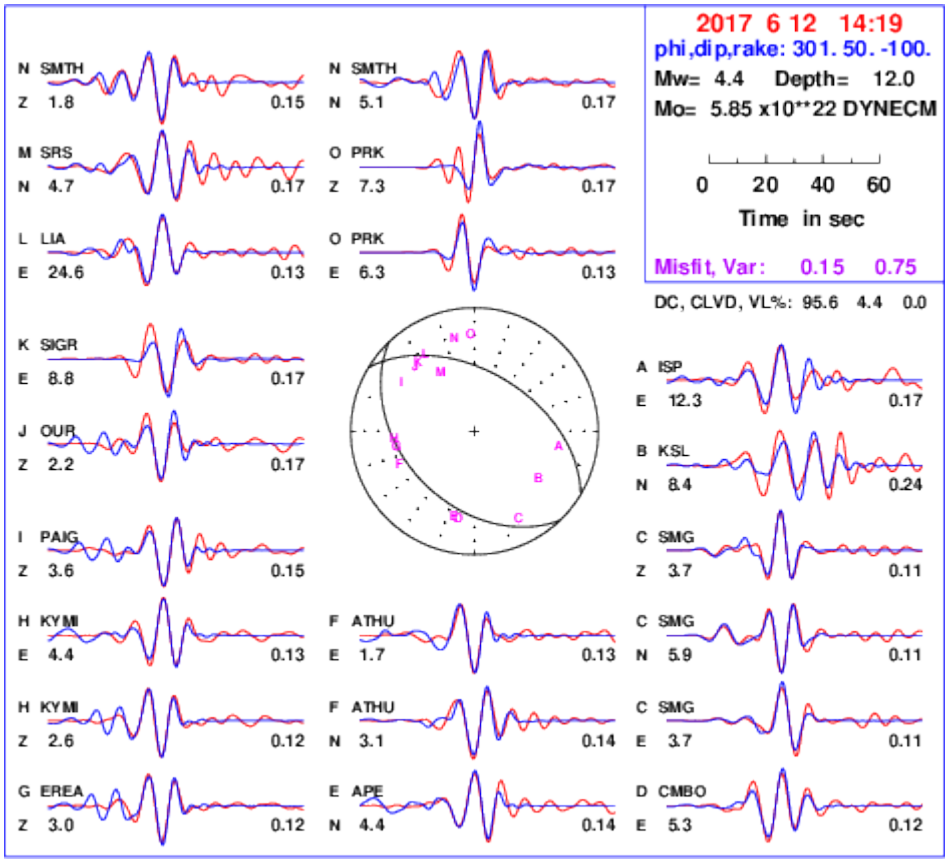

Figure 7: Source parameter determination for a major aftershock that occurred on 12 June 2017 south of Lesvos, using moment tensor inversion and recordings in local and regional distances. Red and blue colour lines represent the observed and synthetic waveforms, respectively.

Coulomb stress analysis was performed, using the source parameters calculated in the framework of the present study, and revealed that the area to the NW was loaded with additional stress of about 0.2 bar (Figure 8).

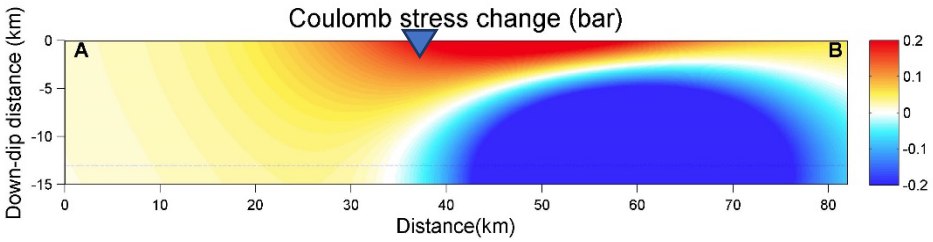

Figure 8: Coulomb stress changes. AB cross-section is parallel to the southern coast of Lesvos Island. The blue triangle indicates the location of Vrissa village.

Preliminary Interferometric Processing

Ground deformation occurred in Lesvos Island during the June 12th seismic event that was determined applying Differential Interferometry. The processing was performed using the SNAP algorithm (http://step.esa.int/main/toolboxes/snap/) incorporated in ESA's Geohazard Thematic Exploitation Platform (https://geohazards-tep.eo.esa.int/). Three SENTINEL-1 Radar images were processed to form two differential interferograms covering the period: May 31st to June 12th, and June 6th to 12th. The common image which was used in both pairs was acquired few hours after the main event (time of acquisition 16:07 GMT). The images of May 31st and June 12th were acquired by S1A satellite, while the image of June 6th was acquired by the S1B satellite. The three radar images were of ascending orbital geometry (Track 131).
The phase for the May 31 to June 12 pair, and June 6 to12 pair is presented in Figure 9. Both images show a fringe of deformation in the central southwestern part of the island and another possible one at the eastern coast. Differences between the two pairs may be attributed to slightly different temporal separation of the master image (May 31 and June 6) and in the slightly different incident angle (33.515^{o} for the May 31 to June 12 pair, and 33.495^{o} for the June 6 to 12 pair).
The SNAPHU algorithm (Chen and Zebker, 2000) was used to unwrap the phase, and estimation of the LOS ground displacement was subsequently performed. The phase was unwrapped successfully mainly in the southern central part of the island, as can be seen in Figure 10. The deformation is along the Line of Sight (LOS) direction. Taking into account the incident angle in the processed area (of about 33.5^{o}), it is evident that a considerable E-W component may be inherent in the data. However, the vertical component is the predominant one; especially considering the type of seismogenic fault (normal fault) revealed by the focal mechanism. The largest deformation is observed in the area around Vrissa Village in the southern part of Lesvos (marked as the eastern dot in the figures). The pair of S1A images (May 31 to June 12) show the strongest deformation in the area of about -6 cm (motion away from the satellite) that is indicative of subsidence, while the second interferometric pair shows smaller deformation of about -3cm.

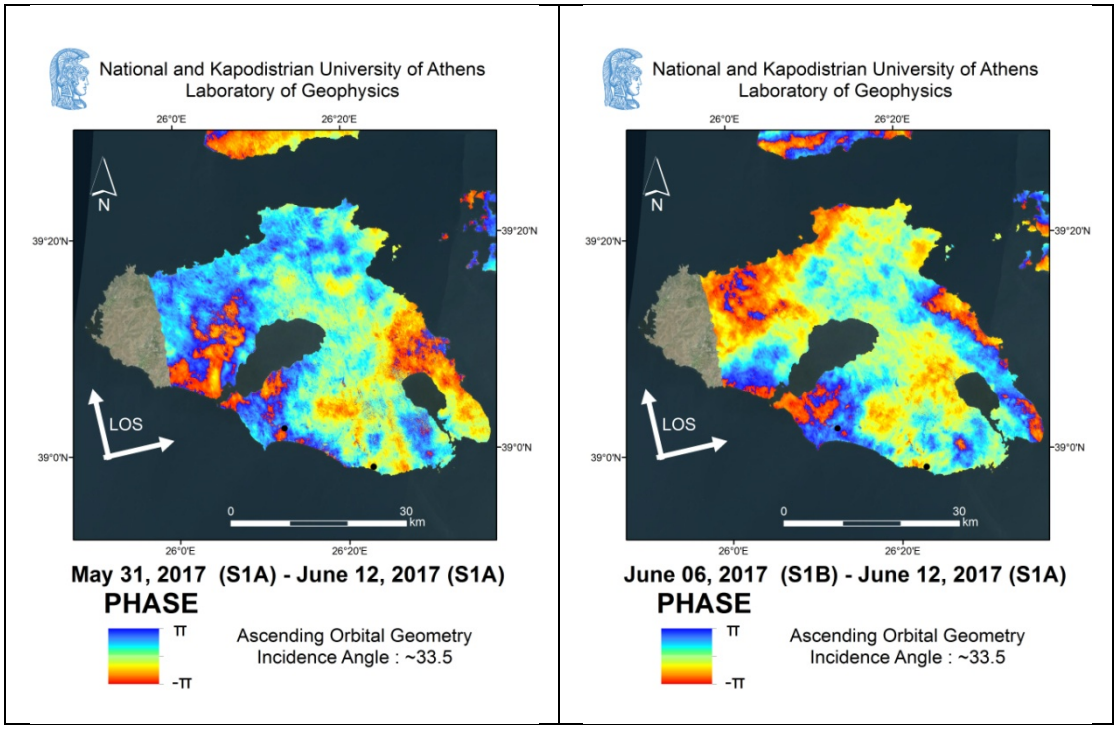

Figure 9: Left: Phase for the first pair of S1A radar images. Black dots in the southern Lesvos donate the position of Vrissa village in the west and Plomari town in the east, which suffers significant damages. Right: Phase for the second pair for the period: June 6 to June 12.

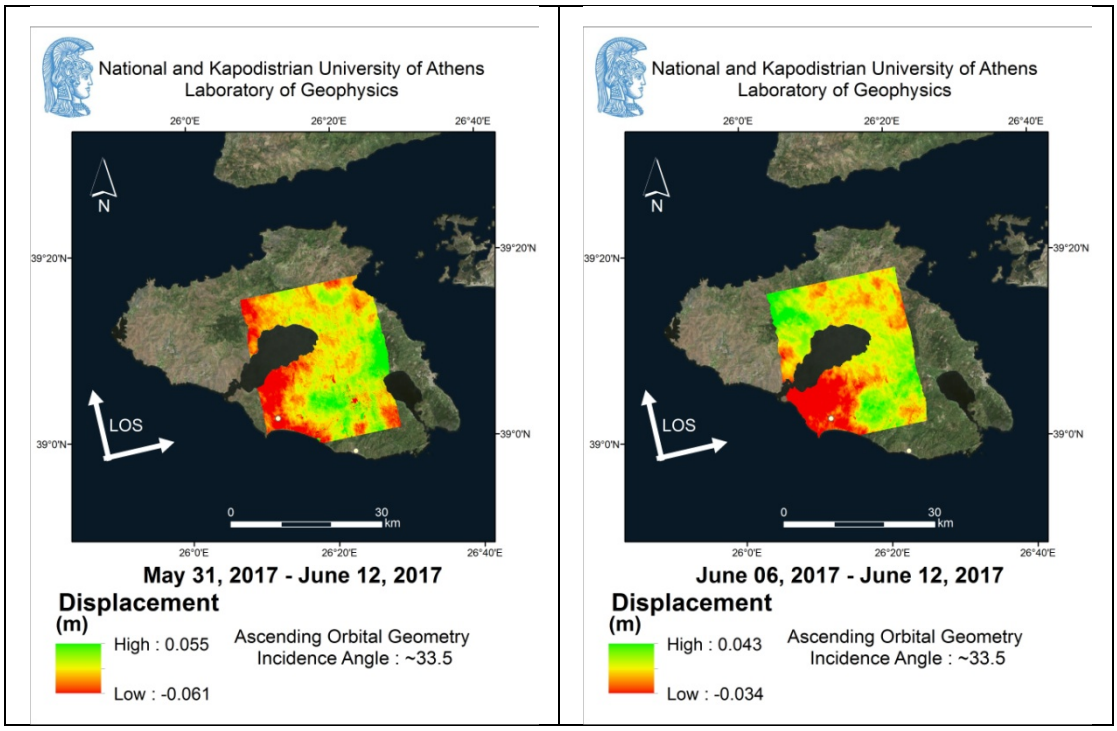

Figure 10: Map showing Ground deformation displacements for the period May 31 to June 12, 2017 (Left image) and for the period June 6 to June 12 (Right image). The displacementsare along the LOS direction. Positive values show motion towards the satellite, while negative values describe motion away from the satellite.

Field Reconnaissance – Polichnitos Fault

During field reconnaissance conducted in the affected area immediately after the earthquake, the onshore tectonic structures were recognized and studied. The main fault of the Vrissa wider area is the NW-SE striking and SW dipping Polichnitos fault. (Figure 11). It is located northeast of the heavily damaged Vrissa settlement and it juxtaposes ophiolites in its footwall against recent deposits comprising Holocene alluvial deposits and Plio-Pleistocene formations in its hanging wall. Along its scarp, fault surfaces (281°/70°, 240°/58°) with kinematic indicators were observed and nearly 1m thick tectonic breccia zone. The measured striations indicate dip- or oblique-slip. Moreover, NW-SE (N310°W) striking surface cracks were also observed disrupting the embankment of a provincial road close and parallel to the Polichnitos fault. They were 50 meters long and 1 cm wide. However, tectonic surface deformation (uplift or subsidence) and associated structures were not detected on both sides of the cracks. Scree formed along the scarp were also detached and rolled down towards the road, while already existing joints in ophiolites were widened.

Figure 11: Partial views of the NW-SE striking and SW-dipping Polichnitos fault. It juxtaposes ophiolites in its footwall (left side) against Quaternary deposits (right side) in both figures.

Drone Flight

The research team conducted a drone flight immediately after the disaster (the next morning) and before any intervention on the site (i.e. debris removal or ruined buildings takedown). The purpose was the construction of a detailed orthomosaic and 3D model (Figure 12) of the affected settlement which would be processed for impact assessment. 440 photos were taken during the flight. The resulting model was ready during the next day and is aiding field reconnaissance and documentation thereafter. Detailed results are going to be presented in following reports.

Figure 12: Up: Partial Digital Surface Model of Vrissa village (using Pix4D Pro software). Irregular surfaces on roads indicate debris - Irregular surfaces within building blocks indicate collapses and other deformations. Down: Orthomosaic of the same area.

Summary

A large earthquake of magnitude M_W = 6.3 occurred on 12 June 2017 south of the SE coast of Lesvos Island, which is located at the NE Aegean, Greece. The source parameters of this event are determined using body-wave modelling. The focal depth was found equal to 13 km, the constrained focal mechanism revealed normal faulting (φ= 293°, δ= 50° and λ= -96°) and the seismic moment 3.5 × 10^{25} dyn cm. The epicentral distribution of the manually analyzed aftershock sequence is aligned along a NW-SE direction, covering an area of about 30x10 km^2. Differential Interferometric processing using SENTINEL 1 radar images, of ascending orbital geometry, showed that the strongest deformation (~3-5 cm on LOS direction) occurred in the southern part of Lesvos island. The type of motion is mainly away from the satellite, consistent to a significant subsiding component.

References

Altinok, Y., Alpar, B., Ozer, N. and Gazioglu, C., 2005. 1881 and 1949 earthquakes at the Chios-Cesme Strait (Aegean Sea) and their relation to tsunamis. Natural Hazards and Earth System Sciences, 5, 717–725.

Barka, A. and Reilinger, R., 1997. Active tectonics of the eastern Mediterranean region: deduced from GPS, neotectonic and seismicity data, Ann. Geofis., XL 3, 587–610.

Bouchon, M., 1979. Discrete wave number representation of elastic wave fields in three-space dimension, J. Geophys. Res., 84, 3609–3614.

Bouchon, M., 2003. A review of the discrete wavenumber method, Pure Appl. Geophys., 160, 445–465.

Chen C. W. and Zebker, H. A., 2000. Network approaches to two-dimensional phase unwrapping: intractability and two new algorithms.' Journal of the Optical Society of America A, 17, 401-414.

Delibasis, N.D. and Voulgaris, N.S., 1989. Microseismic and seismotectonic study of the island of Lesbos. Proc. Fourth Inter. Sem. Res. EC Geothermal Energy Res. And Demo., Florence, 27-30 April 1989, Kluwer Academic Publishers, 474-481.

Dewey, J. F. and Sengör, A. M. C., 1979. Aegean and surrounding regions: complex multiplate and continuum tectonics in a convergent zone, Geol. Soc. Am. Bull., 90, 84–92, doi:10.1130/0016-7606(1979)90<84:AASRCM>2.0.CO;2.

Erkman, H.K., 1949. 23 July 1949 Karaburun (Izmir) Zelzelesi (Le tremlement de terre de Karaburun -Smyrne), Milli Egitim Bakanligi, Istanbul Kandilli Rasathanesi, Sismik Yayinlar:1, Sirketi M¨urettibiye Basimevi, No. 73, Istanbul (in Turkish).

Eyidogan, H., 1988. Rates of crustal deformation in western Turkey as deduced from major earthquakes, Tectonophysics, 148, 83–92.

Hecht, J., 1974. Geological Map of Greece (1:50.000), Lesvos Island, Sheet «Methymna», IGME.

Katsikatsos, G., Mataragas, D., Migiros, G., and Triandafillou, E., 1982. Geological study of Lesbos island, Special Report, IGME.

Kaviris, G., Papadimitriou, P., Kravvariti, Ph., Kapetanidis, V., Karakonstantis, A., Voulgaris, N., Makropoulos, K., 2015. A detailed seismic anisotropy study during the 2011–2012 unrest period in the Santorini Volcanic Complex. Physics of the Earth and Planetary Interiors, 238, 51–88.

Ketin, I., 1948. Uber die tektonischmechanischen Folgerungen aus den grossen anatolischen Erdbeben des letzten Dezenniums. Geologische Rundschau, 36, 77– 83.

Le Pichon, X., Angelier, J., 1979. The Hellenic Arc and trench system: a key to the tectonic evolution of the eastern Mediterranean area. Tectonophysics 60, 1– 42.

Le Pichon, X., Angelier, J., 1981. The Aegean Sea. Philosophical Transactions of the Royal Society of London. A 300, 357–372.

Makropoulos, K., Kaviris, G. and Kouskouna, V., 2012. An updated and extended earthquake catalogue for Greece and adjacent areas since 1900, Nat. Hazards Earth Syst. Sci., 12, 1425-1430.

Mascle, J., Martin, L., 1990. Shallow structure recent evolution of the Aegean Sea: a synthesis based on continuous reflection profiles. Marine Geology 94, 271– 299.

Migiros, G.P., 1992. Introduction to the geology of Lesvos island. 5th Meeting of IGCP Project 276. Chios - Lesvos. Athens Greece, May 25 – 31, 1992.

Papadimitriou, P., Chousianitis, K., Agalos, A., Moshou, A., Lagios, E. and Makropoulos, K., 2012. The spatially extended 2006 April Zakynthos (Ionian Islands, Greece) seismic sequence and evidence for stress transfer, Geophys. Jour. Intern., 190 (2), 1025-1040.

Papadimitriou, P., Kapetanidis, V., Karakonstantis, A., Kaviris, G., Voulgaris, N. and Makropoulos, K., 2015. The Santorini Volcanic Complex: A detailed multi-parameter seismological approach with emphasis on the 2011–2012 unrest period. J. Geodyn., 85, 32–57.

Papazachos, B.C., Papazachou, C., 2003. The Earthquakes of Greece. Ziti Publ., Thessaloniki, Greece.

Papazachos, B.C., Papaioannou Ch., A., Papazachos, C.B. and Savvaidis A.S., 1997. Atlas of isoseismal maps for strong shallow earthquakes in Greece and surrounding area (426BC - 1995). Ziti Publ., Thessaloniki, Greece.

Şengör, A.M.C., Görür, N., Şaroğlu, F., 1985. Strike-slip faulting and related basin formation in zones of tectonic escape: Turkey as a case study. In: Biddle, K.T., Christie- Blick, N. (Eds.). Strike-Slip Faulting and Basin Formation, Soc. Econ. Paleontol. Mineral Spec. Pub., vol. 37. S.E.P.M., Tulsa, OK, 227– 264.

Soulakellis, N., Novak, I., Zouros, N., Lowman, P. and Yates J. 2006. Fusing Landsat-5/TM Imagery and Shaded Relief maps in Tectonic and Geomorphic Mapping: Lesvos Island, Greece. Photogrammetric Engineering and Remote Sensing,72(6), 693-700.

Stucchi, M., Rovida, A., Gomez Capera, A.A., Alexandre, P., Camelbeeck, T., Demircioglu, M.B., Gasperini, P., Kouskouna, V., Musson, R.M.W., Radulian, M., Sesetyan, K., Vilanova, S., Baumont, D., Bungum, H., Fäh, D., Lenhardt, W., Makropoulos, K., Martinez Solares, J.M., Scotti, O.,Zivcic, M., Albini, P., Batllo, J., Papaioannou, C., Tatevossian, R., Locati, M., Meletti, C., Viganò, D., Giardini, D.,

2013. The SHARE European Earthquake Catalog (SHEEC) 1000–18 99, J. Seismolog., 17 (2), 523–544.

Taxeidis K., 2003. Study of Historical Seismicity of the Eastern Aegean Islands. PhD thesis, NKUA, Greece, 301 pp.

Voulgaris, N., Parcharidis, I., Pahoula, M. and Pirlis, E., 2004. Correlation of tectonics, seismicity and geothermics of Lesbos Island using remote sensing data and Geographical Information Systems. Bulletin of the Geological Society of Greece vol. XXXVI, 938-947.

Photos from Vrissa Village


Valera